Fourth-generation standard model imprints in $B \to K^* \ell^+ \ell^-$ decays with polarized K^*

Aqeel Ahmed,[1,*] Ishtiaq Ahmed,[1,†] M. Jamil Aslam,[1,‡] M. Junaid,[1,§] M. Ali Paracha,[1,2,‖] and Abdur Rehman[1,¶]

[1]*National Center for Physics and Physics Department, Quaid-i-Azam University, Islamabad 45320, Pakistan*

[2]*Center for Advance Mathematics and Physics, National University of Science and Technology, Islamabad, Pakistan*

(Received 3 November 2011; published 10 February 2012)

The implication of the fourth-generation quarks in the $B \to K^* \ell^+ \ell^-$ ($\ell = \mu, \tau$) decays when K^* meson is longitudinally or transversely polarized is presented herein. In this context, the dependence of the branching ratio with polarized K^* and the helicity fractions ($f_{L,T}$) of K^* meson were studied. It was observed that the polarized branching ratios as well as helicity fractions are sensitive to the new physics (NP) parameters, especially when the final-state leptons are tauons. Hence, the measurements of these observables at LHC can serve as a good tool to investigate the indirect searches of new physics beyond the standard model.

DOI: 10.1103/PhysRevD.85.034018 PACS numbers: 13.20.He, 14.40.Nd

I. INTRODUCTION

It is well-known that the standard model (SM) with single Higgs boson is the simplest one and that it has been tested with great precision. Despite its many successes, some theoretical shortcomings preclude recognition of this SM as a fundamental theory. For example, this SM does not address the issues of (i) hierarchy puzzle, (ii) origin of mass spectrum, and (iii) *Why only three generations of quarks and leptons?* Neutrinos are massless, but experiments have shown that the neutrinos have nonzero mass.

Issues like those mentioned above indicate that there must be a new physics (NP) beyond the SM. Various extensions of the SM are focused on understanding some of these issues. Some of these extensions are the two Higgs doublet models (2HDM), the minimal supersymmetric SM (MSSM), the universal extra dimension model (UED), and the standard model with fourth-generation (SM4). Extension SM4 implies a fourth family of quarks and leptons, thus it seems to be the most economical in number of additional particles and most simple in the sense that it does not introduce any new operators. Interest in SM4 was fairly high in the 1980s (until the electroweak precision data seemed to rule it out). One reason for this interest in the fourth-generation was the measurement of the number of light neutrinos at the Z pole, which showed only three light neutrinos could exist. However, the discovery of neutrino oscillations suggested the possibility of a mass scale beyond the SM, and the models with sufficiently massive neutrino became acceptable [1]. Though the early study of the electroweak (EW) precision measurements ruled out a fourth-generation [2], it was subsequently pointed out [3] that if the fourth-generation masses are not degenerate then the EW precision data do not prohibit the fourth-generation [4]. Therefore, the SM can be simply extended with a sequential as four-quark and four-lepton left-handed doublets and corresponding right-handed singlets.

The possible sequential fourth-generation may play an important role in understanding the well-known problem of CP violation and flavor structure of standard theory [5–11], electroweak symmetry-breaking [12–15], hierarchies of fermion mass, and mixing angle in quark/lepton sectors [16–20]. A thorough discussion on the theoretical and experimental aspects of fourth-generation can be found in Ref. [21].

It is necessary to mention here that the SM4 particles are heavy in nature, consequently they are hard to produce in the accelerators. Therefore, we have to use alternate scenarios, where we can find their influence at low energies. In this regard, the Flavor Changing Neutral Current (FCNC) transitions provide an ideal plateform to establish new physics (NP) because FCNC transitions are not allowed at tree-level in the SM but allowed at loop-level through the Glashow-Iliopoulos-Maiani mechanism, which can get contributions of NP from newly proposed particles via loop diagrams. Among different FCNC transitions, $b \to s$ transition plays a pivotal role in performing efficient tests of NP scenarios [22–30]. The fact that CP violation in $b \to s$ transitions is predicted to be very small in the SM, thus any experimental evidence for sizable CP-violating effects in the B system would clearly point towards a NP scenario. The FCNC transitions in SM4 contain much fewer parameters and the possibility of having simultaneously sizeable effects in K and B meson systems compared to other NP models.

The exploration of physics beyond the standard model through various inclusive B meson decays like $B \to X_{s,d} \ell^+ \ell^-$ and their corresponding exclusive processes $B \to M \ell^+ \ell^-$ with $M = K, K^*, K_1, \rho$ etc. have been done in literature [31–36]. These studies show that the

*aqeel@ncp.edu.pk
†ishtiaq@ncp.edu.pk
‡jamil@ncp.edu.pk
§mjunaid@ncp.edu.pk
‖ali@ncp.edu.pk
¶rehman@ncp.edu.pk

 © 2012 American Physical Society

mentioned inclusive and exclusive decays of B meson are very sensitive to the flavor structure of the standard model and provide a windowpane for any NP model. There are two different ways to incorporate the NP effects in the rare decays, one through the modification in Wilson coefficients and the other through new operators, which are absent in the standard model. It is necessary to mention here that the FCNC decay modes like $B \to X_s \ell^+ \ell^-$, $B \to K^* \ell^+ \ell^-$, and $B \to K \ell^+ \ell^-$ are also useful in the determination of precise values of $C_7^{\rm eff}$, $C_9^{\rm eff}$, and $C_{10}^{\rm eff}$ Wilson coefficients as well as the sign of $C_7^{\rm eff}$. In particular, these decay modes involved observables that can distinguish between the various extensions of standard model.

The observables like branching ratio, forward-backward asymmetry, lepton polarization asymmetries, and helicity fractions of final state mesons for the semileptonic B decays are greatly influenced under different scenarios beyond the standard model. Therefore, the precise measurement of these observables will play an important role in the indirect searches of NP including SM4. In this work, we study the physical observables, such as branching ratio and helicity fractions when K^* meson is longitudinally and transversely polarized for the decays $B \to K^* \ell^+ \ell^-$ in SM4. The longitudinal helicity fraction f_L has been measured for the K^* meson by LHCb [37], CDF [38], Belle [39], and Babar [40] collaborations for the decay channel $B \to K^* \mu^+ \mu^-$. The recent results are quite intriguing especially those from the LHCb and CDF collaborations. In this respect, it is appropriate to look for observables, which can be tested experimentally in order to pin down the status of SM4. In exclusive decays, the main job is to calculate the form factors. For our analysis, we borrow the light cone QCD sum rules (LCSR) form factors [41].

We have organized our paper as follows: In Sec. II, we fill our toolbox with the theoretical framework needed to study the said process in the fourth-generation SM. In Sec. III, we discuss the phenomenology of the polarized branching ratios and helicity fractions of K^* meson in $B \to K^* \ell^+ \ell^-$ in detail. We also give the numerical analysis of our observables and discuss the sensitivity of these observables with the NP scenarios. We summarize the main points of our findings in Sec. IV.

II. THEORETICAL TOOLBOX

At quark-level the decay $B \to K^* \ell^+ \ell^-$ $(\ell = \mu, \tau)$ is governed by the transition $b \to s \ell^+ \ell^-$ for which the effective Hamiltonian can be written as

$$H_{\rm eff} = -\frac{4G_F}{\sqrt{2}} V_{tb} V_{ts}^* \sum_{i=1}^{10} C_i(\mu) O_i(\mu), \tag{1}$$

where $O_i(\mu)$ $(i = 1, \ldots, 10)$ are the four-quark operators and $C_i(\mu)$ are the corresponding Wilson coefficients at the energy scale μ. The explicit expressions of these in the SM at next-to-leading order and next-to-next-leading order are given in [41–52]. The operators responsible for $B \to K^* \ell^+ \ell^-$ are O_7, O_9, and O_{10} and their form is given by

$$\begin{aligned} O_7 &= \frac{e^2}{16\pi^2} m_b (\bar{s} \sigma_{\mu\nu} P_R b) F^{\mu\nu}, \\ O_9 &= \frac{e^2}{16\pi^2} (\bar{s} \gamma_\mu P_L b)(\bar{l} \gamma^\mu l), \\ O_{10} &= \frac{e^2}{16\pi^2} (\bar{s} \gamma_\mu P_L b)(\bar{l} \gamma^\mu \gamma_5 l), \end{aligned} \tag{2}$$

with $P_{L,R} = (1 \mp \gamma_5)/2$.

In terms of the discussed Hamiltonian, the free-quark decay amplitude for $b \to s\, \ell^+ \ell^-$ in SM4 can be derived as

$$\begin{aligned} \mathcal{M}(b \to s \ell^+ \ell^-) = -\frac{G_F \alpha}{\sqrt{2}\pi} V_{tb} V_{ts}^* \Big\{ & C_9^{\rm eff} (\bar{s} \gamma_\mu L b)(\bar{\ell} \gamma^\mu \ell) \\ & + C_{10} (\bar{s} \gamma_\mu L b)(\bar{\ell} \gamma^\mu \gamma_5 \ell) \\ & - 2 m_b C_7^{\rm eff} \left(\bar{s} i \sigma_{\mu\nu} \frac{q^\nu}{q^2} R b \right) (\bar{\ell} \gamma^\mu \ell) \Big\}, \end{aligned} \tag{3}$$

where q^2 is the square of momentum transfer. The operator O_{10} cannot be induced by the insertion of four-quark operators because of the absence of the Z boson in the effective theory. Therefore, the Wilson coefficient C_{10} does not renormalize under QCD corrections, hence it is independent on the energy scale. In addition to this, the above quark-level decay amplitude can receive contributions from the matrix element of four-quark operators $\sum_{i=1}^{6} \langle \ell^+ \ell^- s | O_i | b \rangle$, which are usually absorbed into the effective Wilson coefficient $C_9^{\rm SM}(\mu)$ and can usually be called $C_9^{\rm eff}$ as found in [35,41]. It is important to emphasis here that the contribution of the long distance usually vetoed effectively in the experimental side, therefore we will not discuss it in the present study.

The sequential fourth-generation model with an additional up-type quark t', down-type quark b', heavy-charged lepton τ', and an associated neutrino ν' is a simple and nonsupersymmetric extension of the SM and, as such, does not add any new dynamics to the SM. Being a simple extension of the SM, it retains all the properties of the SM where the new top-quark t' like the other up-type quarks contributes to $b \to s$ transition at the loop level. Therefore, the effect of fourth-generation displays itself by changing the values of Wilson coefficients $C_7(\mu)$, $C_9(\mu)$, and C_{10} via the virtual exchange of fourth-generation up-type quark t', which then takes the form

$$\lambda_t C_i \to \lambda_t C_i^{\rm SM} + \lambda_{t'} C_i^{\rm new}, \tag{4}$$

where $\lambda_f = V_{fb}^* V_{fs}$ and the explicit forms of the C_i can be obtained from the corresponding expressions of the Wilson coefficients in the SM by substituting $m_t \to m_{t'}$. By adding an extra family of quarks, the Cabibbo Kobayashi Maskawa (CKM) quark-mixing matrix of the SM is extended by another row and column, which now becomes 4×4. The unitarity of which leads to

$$\lambda_u + \lambda_c + \lambda_t + \lambda_{t'} = 0.$$

Since $\lambda_u = V_{ub}^* V_{us}$ has a very small value compared to the others, we will ignore it. From $\lambda_t \approx -\lambda_c - \lambda_{t'}$ and Eq. (4) we have

$$\lambda_t C_i^{\rm SM} + \lambda_{t'} C_i^{\rm new} = -\lambda_c C_i^{\rm SM} + \lambda_{t'}(C_i^{\rm new} - C_i^{\rm SM}). \quad (5)$$

One can clearly see that under $\lambda_{t'} \to 0$ or $m_{t'} \to m_t$ the term $\lambda_{t'}(C_i^{\rm new} - C_i^{\rm SM})$ vanishes, which is the requirement of the Glashow-Iliopoulos-Maiani mechanism. Taking the contribution of the t' quark in the loop, the Wilson coefficients C_i can be written in the following form:

$$\begin{aligned} C_7^{\rm tot}(\mu) &= C_7^{\rm eff\ SM}(\mu) + \frac{\lambda_{t'}}{\lambda_t} C_7^{\rm new}(\mu), \\ C_9^{\rm tot}(\mu) &= C_9^{\rm eff\ SM}(\mu) + \frac{\lambda_{t'}}{\lambda_t} C_9^{\rm new}(\mu), \\ C_{10}^{\rm tot}(\mu) &= C_{10}^{\rm SM}(\mu) + \frac{\lambda_{t'}}{\lambda_t} C_{10}^{\rm new}(\mu), \end{aligned} \quad (6)$$

where we factored out $\lambda_t = V_{tb}^* V_{ts}$ term in the effective Hamiltonian given in Eq. (1); the last term in these expressions corresponds to the contribution of the t' quark to the Wilson Coefficients. $\lambda_{t'}$ can be parameterized as

$$\lambda_{t'} = |V_{t'b}^* V_{t's}| e^{i\phi_{sb}}, \quad (7)$$

where ϕ_{sb} is the new CP-odd phase.

Parametrization of the Matrix Elements and Form Factors

The exclusive $B \to K^* \ell^+ \ell^-$ decay involves the hadronic matrix elements, which can be obtained by sandwiching the quark-level operators given in Eq. (6) between initial state B meson and final state K^* meson. These can be parameterized in terms of the form factors, which are the scalar functions of the square of the four-momentum transfer ($q^2 = (p-k)^2$). The nonvanishing matrix elements for the process $B \to K^*$ can be parameterized in terms of the seven-form factors as follows:

$$\langle K^*(k,\varepsilon)|\bar{s}\gamma_\mu b|B(p)\rangle = \epsilon_{\mu\nu\alpha\beta}\varepsilon^{*\nu} p^\alpha k^\beta \frac{2A_V(q^2)}{M_B + M_{K^*}} \quad (8)$$

$$\begin{aligned} &\langle K^*(k,\varepsilon)|\bar{s}\gamma_\mu\gamma_5 b|B(p)\rangle \\ &\quad = i\varepsilon_\mu^*(M_B + M_{K^*})A_1(q^2) \\ &\qquad - i(\varepsilon^*\cdot q)(p+k)_\mu \frac{A_2(q^2)}{M_B + M_{K^*}} \\ &\qquad - i2(\varepsilon^*\cdot q) q_\mu M_{K^*} \frac{A_3(q^2) - A_0(q^2)}{q^2}, \end{aligned} \quad (9)$$

where p is the momentum of B meson and ε (k) are the polarization vector (momentum) of the final state K^* meson. In Eq. (9) we use the following exact relation:

$$A_3(q^2) = \frac{M_B + M_{K^*}}{2M_{K^*}} A_1(q^2) - \frac{M_B - M_{K^*}}{2M_{K^*}} A_2(q^2) \quad (10)$$

with

$$A_3(0) = A_0(0).$$

In addition to the above form factors, Eqs. (8) and (9), there are some penguin-form factors, which we can write as

$$\langle K^*(k,\varepsilon)|\bar{s}\sigma_{\mu\nu} q^\nu b|B(p)\rangle = 2i\epsilon_{\mu\nu\alpha\beta}\varepsilon^{*\nu} p^\alpha k^\beta T_1(q^2) \quad (11)$$

$$\begin{aligned} &\langle K^*(k,\varepsilon)|\bar{s}\sigma_{\mu\nu} q^\nu \gamma^5 b|B(p)\rangle \\ &\quad = \{(M_B^2 - M_{K^*}^2)\varepsilon_\mu^* - (\varepsilon^*\cdot q)(p+k)_\mu\} T_2(q^2) \\ &\qquad + (\varepsilon^*\cdot q)\left\{q_\mu - \frac{q^2}{M_B^2 - M_{K^*}^2}(p+k)_\mu\right\} T_3(q^2). \end{aligned} \quad (12)$$

The form factors $A_V(q^2)$, $A_1(q^2)$, $A_2(q^2)$, $A_3(q^2)$, $A_0(q^2)$, $T_1(q^2)$, $T_2(q^2)$, $T_3(q^2)$ are the nonperturbative quantities and to calculate them one has to rely on some nonperturbative approaches. To study the physical observables, we take the form factors calculated in the framework of LCSR [41]. The dependence of the form factors on the square of the momentum transfer (q^2) can be written as

$$F(q^2) = F(0) Exp\left[c_1 \frac{q^2}{M_B^2} + c_2 \frac{q^4}{M_B^4}\right], \quad (13)$$

where the values of the parameters $F(0)$, c_1, and c_2 are given in Table I.

Now in terms of these form factors and from Eq. (3) the penguin amplitude can be straightforwardly written as

$$\mathcal{M} = -\frac{G_F \alpha}{2\sqrt{2}\pi} V_{tb} V_{ts}^* [\mathcal{T}_\mu^1 (\bar{l}\gamma^\mu l) + \mathcal{T}_\mu^2 (\bar{l}\gamma^\mu\gamma^5 l)],$$

where

TABLE I. $B \to K^*$ form factors corresponding to penguin contributions in the light cone QCD Sum Rules. $F(0)$ denotes the value of form factors at $q^2 = 0$ while c_1 and c_2 are the parameters in the parametrization shown in Eq. (13) [41].

$F(q^2)$	$F(0)$	c_1	c_2
$A_V(q^2)$	$0.457^{+0.091}_{-0.058}$	1.482	1.015
$A_1(q^2)$	$0.337^{+0.048}_{-0.043}$	0.602	0.258
$A_2(q^2)$	$0.282^{+0.038}_{-0.036}$	1.172	0.567
$A_0(q^2)$	$0.471^{+0.227}_{-0.059}$	1.505	0.710
$T_1(q^2)$	$0.379^{+0.058}_{-0.045}$	1.519	1.030
$T_2(q^2)$	$0.379^{+0.058}_{-0.045}$	0.517	0.426
$T_3(q^2)$	$0.260^{+0.035}_{-0.026}$	1.129	1.128

$$\mathcal{T}^1_\mu = f_1(q^2)\epsilon_{\mu\nu\alpha\beta}\varepsilon^{*\nu}p^\alpha k^\beta - if_2(q^2)\varepsilon^*_\mu + if_3(q^2)(\varepsilon^*\cdot q)P_\mu \tag{14}$$

$$\mathcal{T}^2_\mu = f_4(q^2)\epsilon_{\mu\nu\alpha\beta}\varepsilon^{*\nu}p^\alpha k^\beta - if_5(q^2)\varepsilon^*_\mu + if_6(q^2)(\varepsilon^*\cdot q)P_\mu + if_0(q^2)(\varepsilon^*\cdot q)q_\mu. \tag{15}$$

The functions f_0 to f_6 in Eqs. (14) and (15) are known as auxiliary functions, which contain both long-distance (form factors) and short-distance (Wilson coefficients) effects and these can be written as

$$f_1(q^2) = 4(m_b+m_s)\frac{C_7^{\rm tot}}{q^2}T_1(q^2) + 2C_9^{\rm tot}\frac{A_V(q^2)}{M_B+M_{K^*}} \tag{16a}$$

$$f_2(q^2) = \frac{2C_7^{\rm tot}}{q^2}(m_b-m_s)T_2(q^2)(M_B^2-M_{K^*}^2) + C_9^{tot}A_1(q^2)(M_B+M_{K^*}) \tag{16b}$$

$$f_3(q^2) = 4\frac{C_7^{\rm tot}}{q^2}(m_b-m_s)\left(T_2(q^2)+q^2\frac{T_3(q^2)}{(M_B^2-M_{K^{*2}})}\right) + 2C_9^{\rm tot}\frac{A_2(q^2)}{M_B+M_{K^*}} \tag{16c}$$

$$f_4(q^2) = C_{10}^{\rm tot}\frac{2A_V(q^2)}{M_B+M_{K^*}} \tag{16d}$$

$$f_5(q^2) = C_{10}^{\rm tot}A_1(q^2)(M_B+M_{K^*}) \tag{16e}$$

$$f_6(q^2) = C_{10}^{\rm tot}\frac{A_2(q^2)}{M_B+M_{K^*}} \tag{16f}$$

$$f_0(q^2) = C_{10}^{\rm tot}\frac{A_3(q^2)-A_0(q^2)}{M_B+M_{K^*}}. \tag{16g}$$

III. PHENOMENOLOGICAL OBSERVABLES

A. Polarized Branching Ratio

The explicit expression of the differential decay rate for $B\to K^*\ell^+\ell^-$, when the K^* meson is polarized can be written in terms of longitudinal Γ_L and transverse components Γ_T as [36]

$$\frac{d\Gamma_L(q^2)}{dq^2} = \frac{G_F^2|V_{tb}V_{ts}^*|^2\alpha^2}{2^{11}\pi^5}\frac{u(q^2)}{M_B^3}\times\frac{1}{3}\mathcal{A}_L \tag{17}$$

$$\frac{d\Gamma_\pm(q^2)}{dq^2} = \frac{G_F^2|V_{tb}V_{ts}^*|^2\alpha^2}{2^{11}\pi^5}\frac{u(q^2)}{M_B^3}\times\frac{4}{3}\mathcal{A}_\pm \tag{18}$$

$$\frac{d\Gamma_T(q^2)}{dq^2} = \frac{d\Gamma_+(q^2)}{dq^2} + \frac{d\Gamma_-(q^2)}{dq^2}. \tag{19}$$

The longitudinal (transverse)-differential branching ratios $BR_L(BR_T)$ are plotted in Figs. 1 and 2 as a function of q^2.

The kinematical variables used in Eqs. (17)–(19) are defined as

$$u(q^2) \equiv \sqrt{\lambda\left(1-\frac{4m_\ell^2}{q^2}\right)} \tag{20}$$

with

$$\lambda \equiv \lambda(m_B^2, m_{K^*}^2, q^2) = m_B^4 + m_{K^*}^4 + q^4 - 2m_{K^*}^2m_B^2 - 2q^2m_B^2 - 2q^2m_{K^*}^2. \tag{21}$$

The different functions appearing in Eqs. (17) and (18) can be expressed in terms of auxiliary functions [c.f. Eqs (16a)–(16g)] as

$$\mathcal{A}_L = \frac{1}{q^2M_{K^*}}[24|f_0(q^2)|^2m^2M_{K^*}^2\lambda + 2(2m^2+q^2)|(M_B^2-M_{K^*}^2-q^2)f_2(q^2) + \lambda f_3(q^2)|^2 + (q^2-4m^2)|(M_B^2-M_{K^*}^2-q^2)f_5(q^2) + \lambda f_6(q^2)|^2] \tag{22}$$

$$\mathcal{A}_\pm = (q^2-4m^2)|f_5(q^2) \mp \sqrt{\lambda}f_4(q^2)|^2 + (q^2+2m^2)|f_2(q^2) \mp \sqrt{\lambda}f_1(q^2)|^2, \tag{23}$$

where m is the mass of lepton.

B. Helicity Fractions of K^* Meson

We now discuss helicity fractions of K^* in $B\to K^*\ell^+\ell^-$, which are interesting observables and that are independent of the uncertainties that arise due to form factors and other input parameters. The final-state meson helicity fractions were already discussed in literature for $B\to K^*(K_1)\ell^+\ell^-$ decays [34,35,53,54]. The longitudinal helicity fraction f_L has been measured for the K^*-vector meson by the LHCb [37], CDF [38], Belle [39], and Babar [40] collaborations for the decay $B\to K^*\ell^+\ell^-(l=e,\mu)$ in the region of low-momentum transfer ($0.1\le q^2\le 6$ GeV^2). The results are given as

$$f_L = 0.57^{+0.11}_{-0.10}\pm 0.03, \quad \text{(LHCb)} \tag{24a}$$

$$f_L = 0.69^{+0.19}_{-0.21}\pm 0.08, \quad \text{(CDF)} \tag{24b}$$

$$f_L = 0.67^{+0.23}_{-0.23}\pm 0.05, \quad \text{(Belle)} \tag{24c}$$

$$f_L = 0.35^{+0.16}_{-0.16}\pm 0.04, \quad \text{(Babar)}, \tag{24d}$$

while the SM average value of f_L in $0.1\le q^2\le 6$ GeV^2) range is $f_L = 0.65$, where the average value of the helicity fractions is defined as

$$\langle f_{L,T}\rangle = \frac{\int_{q^2_{\rm min}}^{q^2_{\rm max}} f_{L,T}(q^2)\frac{dBR_{L,T}}{dq^2}dq^2}{\int_{q^2_{\rm min}}^{q^2_{\rm max}}\frac{dBR_{L,T}}{dq^2}dq^2}, \tag{25}$$

where $q^2_{\rm min} = 4m_\ell^2$ and $q^2_{\rm max} = (M_B^2 - M_K^{*2})$.

Finally, the longitudinal and transverse helicity amplitude becomes

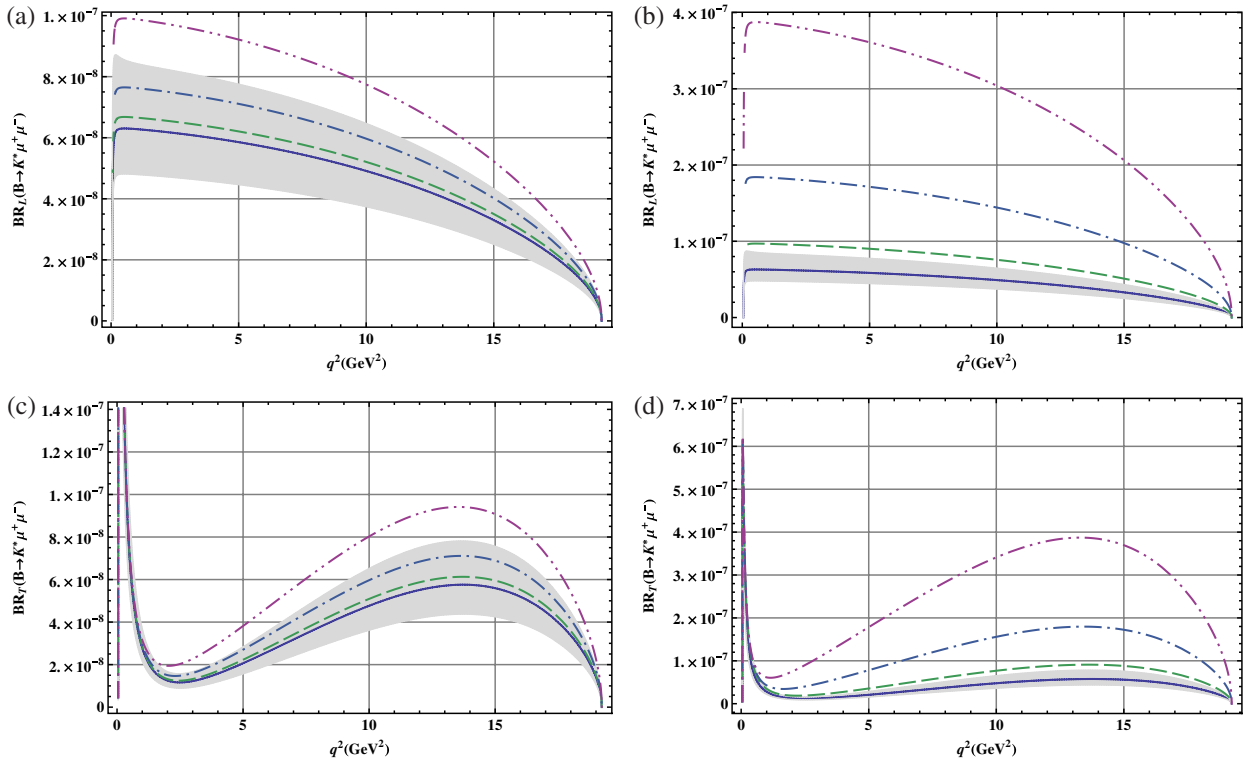

FIG. 1 (color online). The dependence of the longitudinal and transverse BR for the decay $B \to K^*(892)\mu^+\mu^-$ on q^2 for different values of $m_{t'}$ and $|V^*_{t'b}V_{t's}|$. In all the graphs, the solid line corresponds to the SM, dashed, dashed-dot, and dashed-double dot corresponds to $m_{t'} = 300$ GeV, 450 GeV, and 600 GeV, respectively. $|V^*_{t'b}V_{t's}|$ has the value 0.005 and 0.015 in (a) and (b), respectively.

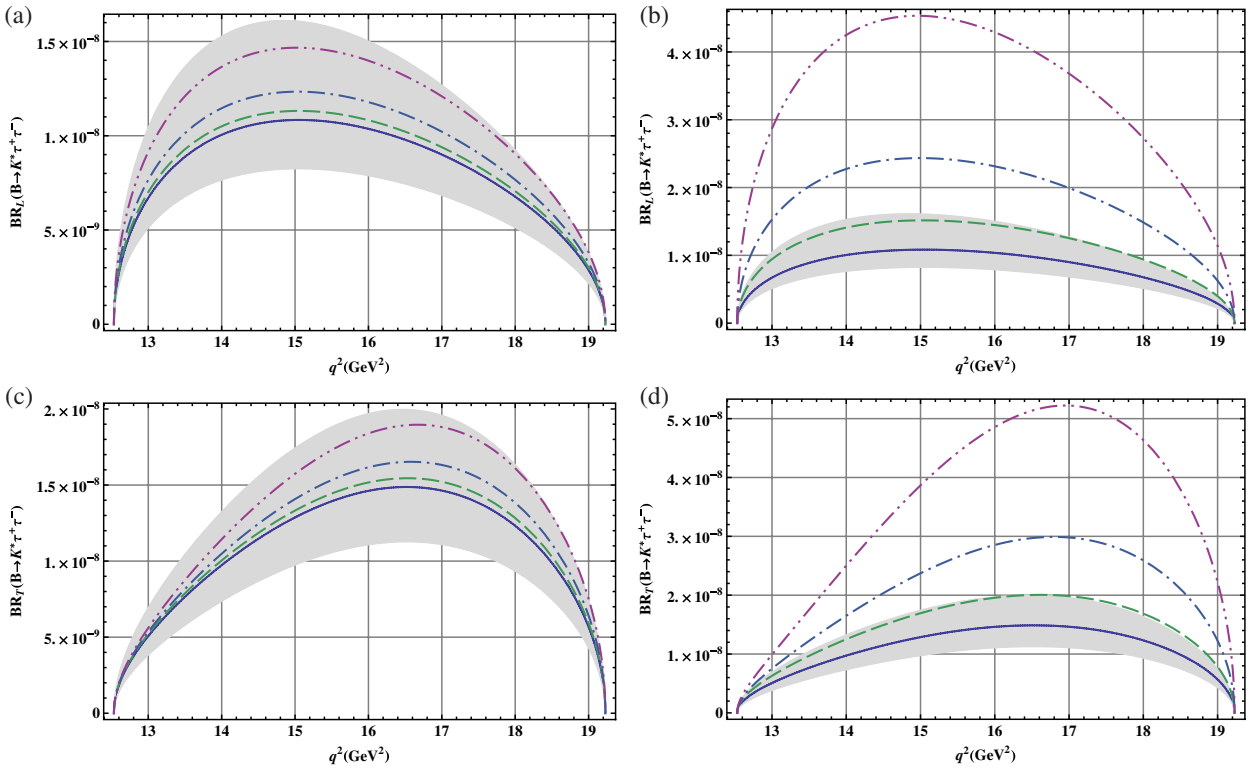

FIG. 2 (color online). The dependence of the longitudinal and transverse BR for the decay $B \to K^*(892)\tau^+\tau^-$ on q^2 for different values of $m_{t'}$ and $|V^*_{t'b}V_{t's}|$. Legends and the values of the fourth-generation parameters are the same as in Fig. 1.

TABLE II. Default values of input parameters used in the calculations [55].

$m_B = 5.28$ GeV, $m_b = 4.28$ GeV, $m_\mu = 0.105$ GeV,
$m_\tau = 1.77$ GeV, $f_B = 0.25$ GeV, $\lvert V_{tb}V_{ts}^*\rvert = 45 \times 10^{-3}$,
$\alpha^{-1} = 137$, $G_F = 1.17 \times 10^{-5}$ GeV^{-2},
$\tau_B = 1.54 \times 10^{-12}$ sec, $m_{K^*} = 0.892$ GeV.

TABLE III. The Wilson coefficients C_i^μ at the scale $\mu \sim m_b$ in the SM [41].

C_1	C_2	C_3	C_4	C_5	C_6	C_7	C_9	C_{10}
1.107	−0.248	−0.011	−0.026	−0.007	−0.031	−0.313	4.344	−4.669

$$f_L(q^2) = \frac{d\Gamma_L(q^2)/dq^2}{d\Gamma(q^2)/dq^2} \qquad f_\pm(q^2) = \frac{d\Gamma_\pm(q^2)/dq^2}{d\Gamma(q^2)/dq^2}$$
$$f_T(q^2) = f_+(q^2) + f_-(q^2), \tag{26}$$

so that the sum of the longitudinal and transverse helicity amplitudes is equal to 1 i.e. $f_L(q^2) + f_T(q^2) = 1$ for each value of q^2 [34].

C. Numerical Work and Discussion

In this section we analyze the impact of SM4 on the observables like longitudinal branching ratio (BR_L), transverse branching ratio (BR_T), and helicity fractions of K^* for $B \to K^*\ell^+\ell^-$ ($\ell = \mu, \tau$) decays. In the numerical calculation of the said physical observables, the LCSR-form factors are used and given in Table I; other input parameters are collected in Table II; the values of Wilson coefficients are given in Table III.

Before we discuss the numerical analysis, we need to mention here that the shaded regions in all the figures are due to the uncertainties in the form factors. Moreover, from Figs. 3 and 4 we have performed integration over q^2 in fully available phase-space region.

1. NP in Polarized branching ratios BR_L and BR_T

(i) In Figs. 1 and 2 we plotted the differential longitudinal and transverse-differential branching ratios BR_L and BR_T as a function of q^2 for μ and τ as final-state leptons for the said decay. In these graphs, we set the value $\phi_{sb} = 90°$ and vary the values of $m_{t'}$ and $\lvert V_{t'b}V_{t's}\rvert$ such that they lie well within the constraints obtained from different B meson decays [56]. These graphs indicate that both BR_L and BR_T are increasing functions of the SM4 parameters. One can also see that at the minimum values of the SM4 parameters, the NP effects are masked by the uncertainties, especially for the tauons as final-state leptons. However, when we set the maximum values of these parameters, the increment in both the BR_L and BR_T, lie well above the uncertainties in the SM values, as shown in Figs. 1 and 2.

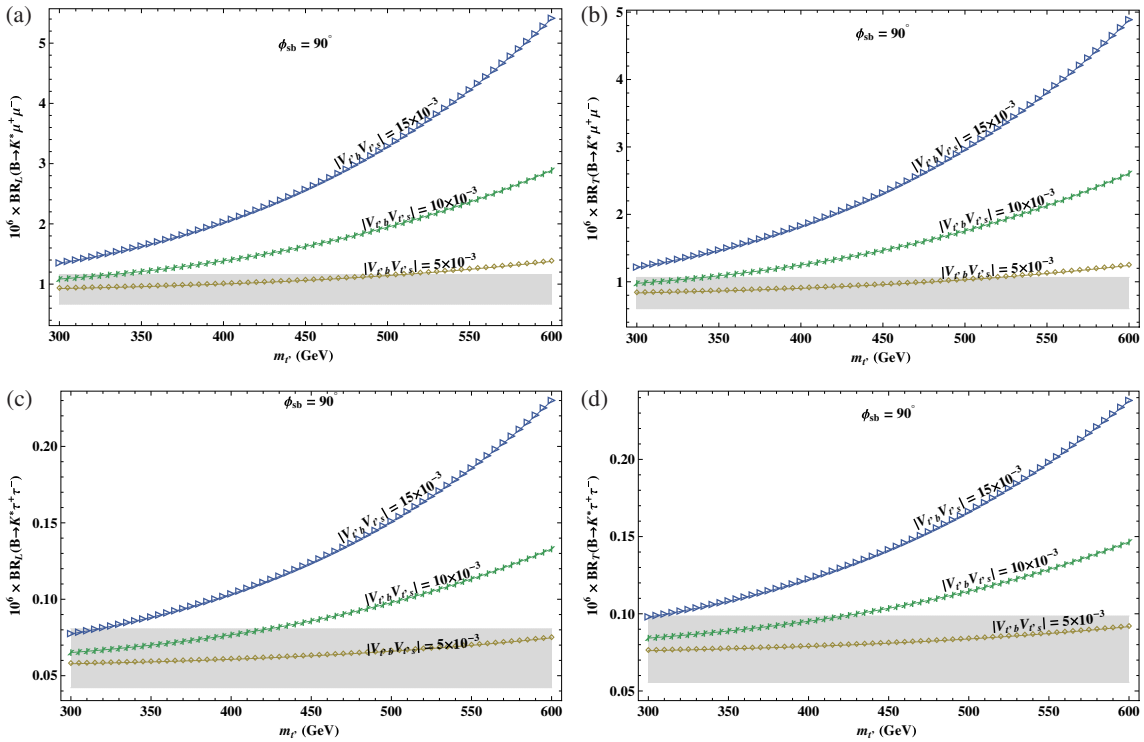

FIG. 3 (color online). The dependence of the total longitudinal and transverse BR for the decay $B \to K^*(892)\mu^+\mu^-$ on $m_{t'}$ for different values of $\lvert V_{t'b}^* V_{t's}\rvert$.

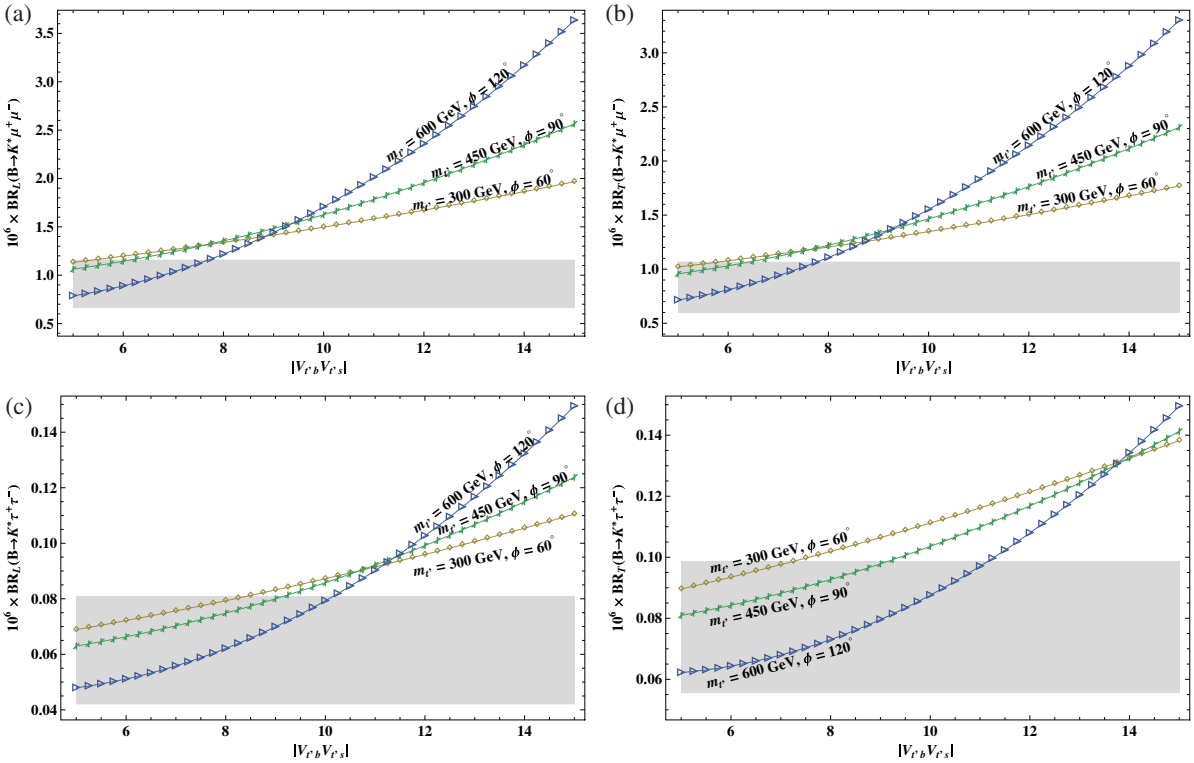

FIG. 4 (color online). The dependence of the total longitudinal and transverse BR for the decay $B \to K^*(892)\mu^+\mu^-$ on $|V^*_{t'b}V_{t's}|$ for different values of $m_{t'}$.

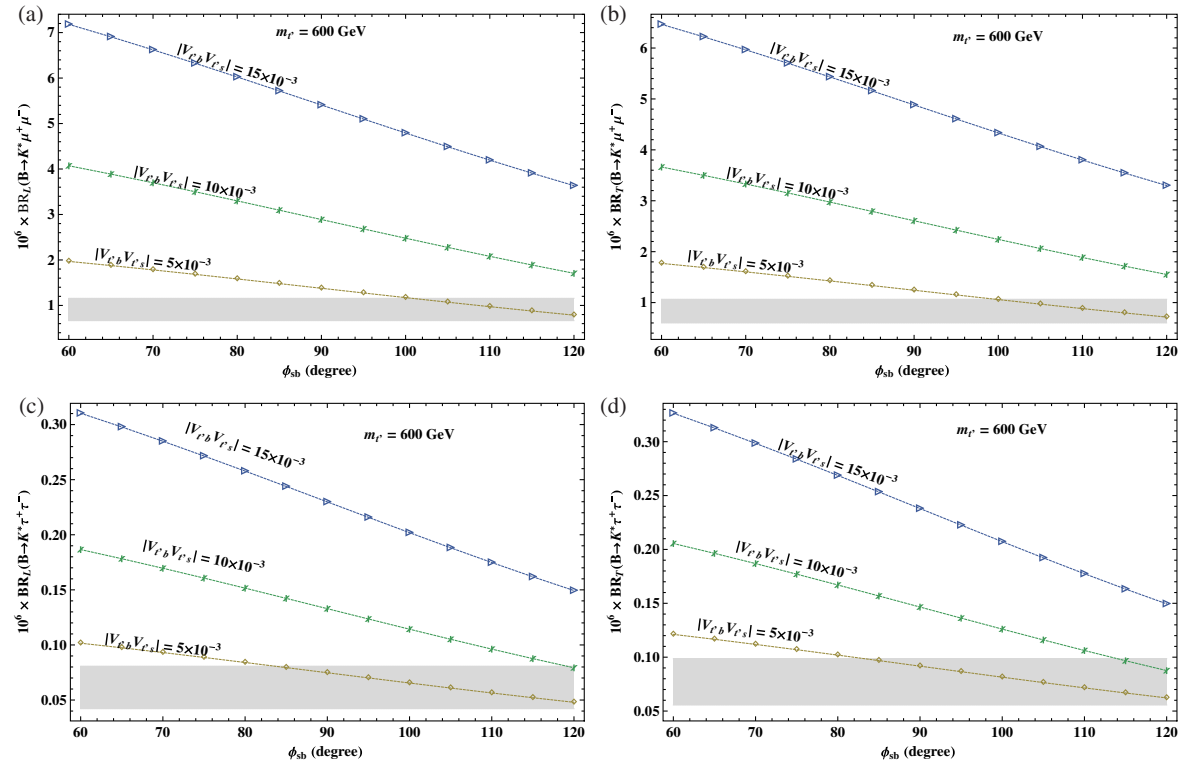

FIG. 5 (color online). The dependence of the total longitudinal and transverse BR for the decay $B \to K^*(892)\mu^+\mu^-$ on ϕ_{sb} for different values of $m_{t'}$ and $|V^*_{t'b}V_{t's}|$.

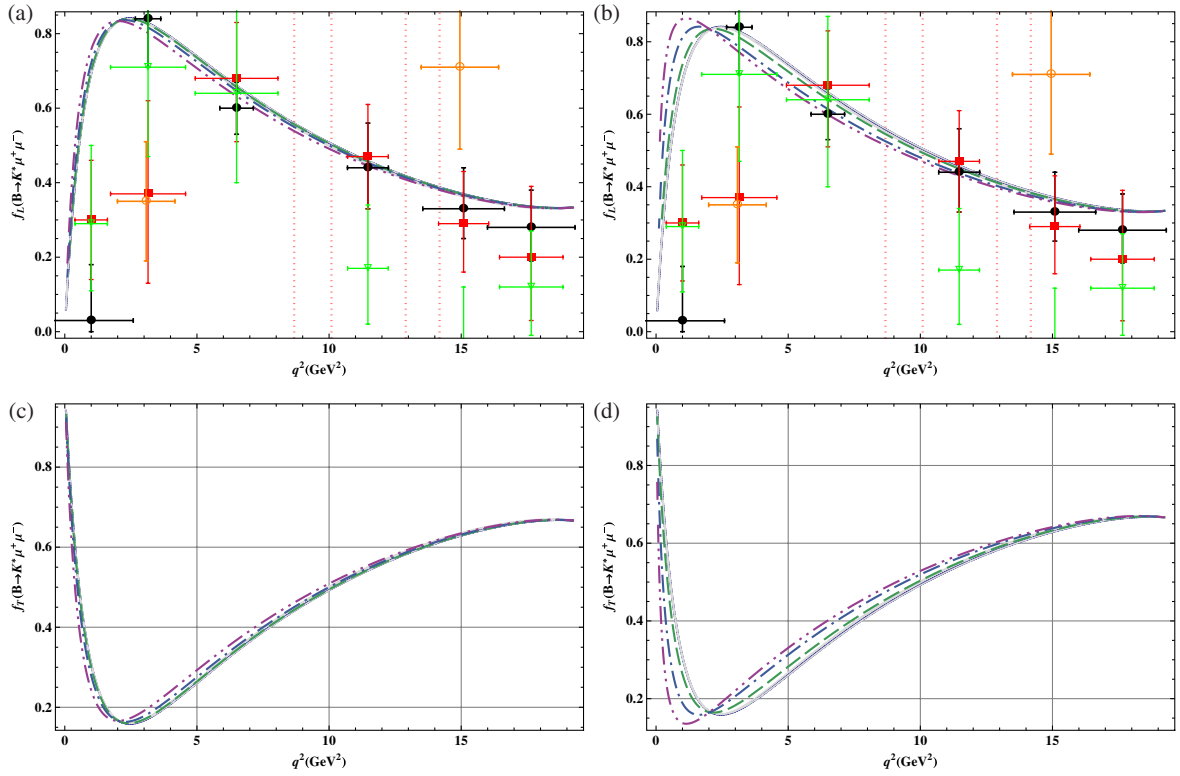

FIG. 6 (color online). The dependence of the longitudinal and transverse helicity fractions for the decay $B \to K^*(892)\mu^+\mu^-$ on q^2 for different values of $m_{t'}$ and $|V^*_{t'b}V_{t's}|$. Legends and the values of the fourth-generation parameters are the same as in Fig. 1 while in the graphs in (a) and (b) the data points • (black), ■ (red), ▽ (green) and ⊕ (orange) correspond to the LHCb [37], CDF [38], Belle [39] and Babar [40] collaborations, respectively.

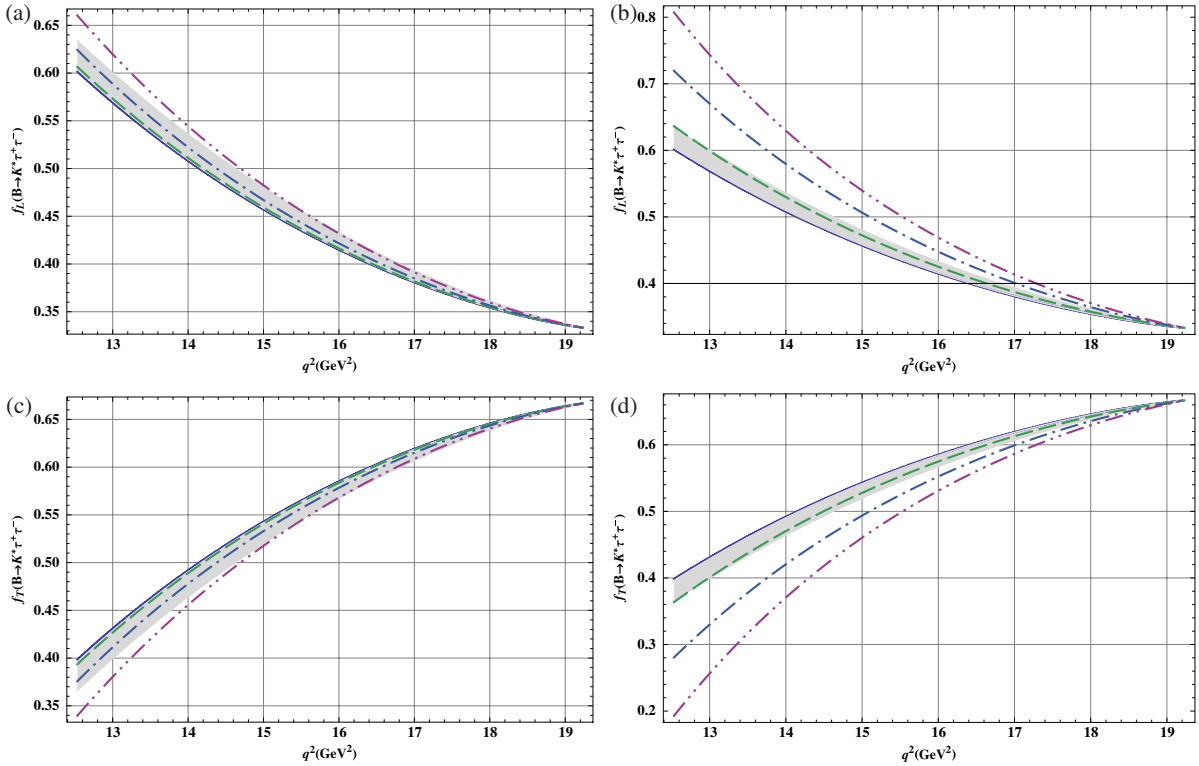

FIG. 7 (color online). The dependence of the longitudinal and transverse helicity fractions for the decay $B \to K^*(892)\tau^+\tau^-$ on q^2 for different values of $m_{t'}$ and $|V^*_{t'b}V_{t's}|$. Legends and the values of the fourth-generation parameters are the same as in Fig. 1.

TABLE IV. Average longitudinal helicity fraction $\langle f_L \rangle$ of K^* meson for different values of $m_{t'}$ and $|V_{t'b}V_{t's}^*|$, whereas $\langle f_L^{\rm SM} \rangle = 0.649$.

$m_{t'}$	$\lvert V_{t'b}V_{t's}^*\rvert = 5 \times 10^{-3}$	$\lvert V_{t'b}V_{t's}^*\rvert = 15 \times 10^{-3}$
300	0.653	0.675
450	0.666	0.715
600	0.685	0.740

(ii) To see the explicit dependence on the SM4 parameters, we have integrated-out BR_L and BR_T over q^2 and have drawn both of them against the $m_{t'}$, $|V_{t'b}V_{t's}|$ and ϕ_{sb} in Figs. 3–5. In Fig. 3, we have plotted BR_L and BR_T vs $m_{t'}$, where ϕ_{sb} is set to be 90° and three different values of $|V_{t'b}V_{t's}|$ are chosen (i.e 0.005, 0.01, and 0.015). These graphs clearly depict that as the value of $m_{t'}$ is increased the BR_L and BR_T are enhanced accordingly. For the case of muons as a final-state leptons (see Figs. 3(a) and 3(b)), the increment in the BR_L and BR_T values at the maximum value of $m_{t'} =$ 600 GeV is up to 5 times that of the SM values; in the case of tauns, which is presented in Figs. 3(c) and 3(d), the increment in the BR_L and BR_T values is approximately 3–4 times larger than that of the SM values.

(iii) In Fig. 4, BR_L and BR_T are plotted as a function of $|V_{t'b}V_{t's}|$, where three different curves correspond to the three different values of $m_{t'} = 300$, 450, 600 GeV, and $\phi_{sb} = 60°, 90°, 120°$ as shown in the graphs. From these graphs one can easily see that similar to the case of $m_{t'}$, the BR_L and BR_T are also an increasing function of $|V_{t'b}V_{t's}|$.

(iv) Variation in SM4 Cabibo Kobayashi Maskawa matrix (CKM4) phase ϕ_{sb}. We plotted BR_L and BR_T vs ϕ_{sb} in Fig. 5. We noticed that in contrast to the previous two cases for $m_{t'}$ and $|V_{t'b}V_{t's}|$, the BR_L and BR_T are increasing when ϕ_{sb} is decreasing. It is easy to extract from the graph that at $\phi_{sb} = 60°$, $m_{t'} = 600$ GeV and $|V_{t'b}V_{t's}| = 0.015$, the values of BR_L and BR_T are about 6–7 times larger than that of their SM values both for muons and tauons. Furthermore, the branching ratio (BR) for each value of $|V_{t'b}V_{t's}|$ decreases to almost half when ϕ_{sb} reaches 120° (Fig. 5).

2. NP in helicity fractions f_L and f_T

(i) As for the study of the polarization of the final-state meson, K^* is concerned in the $B \to K^* l^+ l^-$ decay channel, the longitudinal f_L and transverse f_T helicity fractions become important observables since the uncertainty in this observable is almost negligible, especially when we have muons as the final-state leptons. The helicity fraction is the probability of longitudinally and transversely polarized K^* meson in the above decay channel, so their sum should be equal to 1, which can be seen in Figs. 6 and 7. Moreover, in Figs. 6(a) and 6(b) we have punched the data points • (black), ■ (red), ▽ (green), and ⊕ (orange) corresponding to the LHCb [37], CDF [38], Belle [39], and Babar [40] collaborations, respectively.

(ii) In Fig. 6, f_L and f_T as a function of $q^2(\text{GeV}^2)$ for muons as final-state leptons are plotted. Here, to check the influence of SM4 on the f_L and f_T, we set $\phi_{sb} = 90°$ and vary the values of $m_{t'}$ and $|V_{t'b}V_{t's}|$. Plots (6a) and (6b) depict that at the minimum value of $m_{t'} = 300$ GeV, the effects in helicity fraction are negligible, while at the maximum value of $m_{t'} = 600$ GeV the effects are mild. Whereas the recent results, especially from the LHCb and CDF collaboration, are favoring the SM predictions as shown in Figs. 6(a) and 6(b), and one can also see that the corresponding SM4 curves are very close to some of the data points; the deviation to the SM curve is also not robust so the helicity fraction for the case of muons is not a

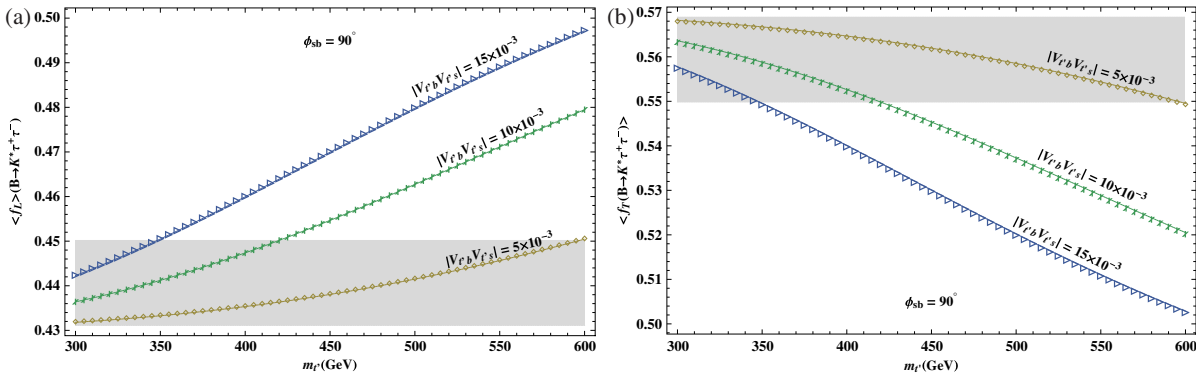

FIG. 8 (color online). The dependence of the average longitudinal helicity fraction for the decay $B \to K^*(892)\tau^+\tau^-$ on $m_{t'}$ and ϕ_{sb} for different values of $|V_{t'b}^* V_{t's}|$.

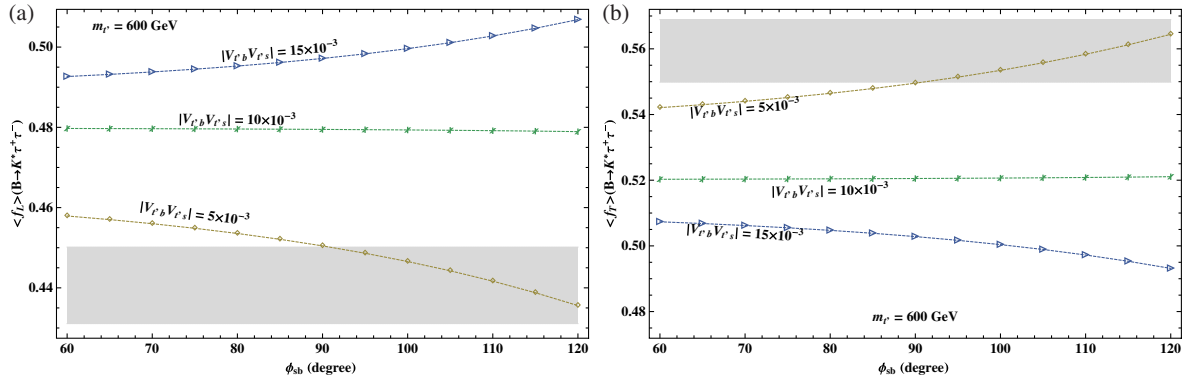

FIG. 9 (color online). The dependence of the average transverse helicity fraction for the decay $B \to K^*(892)\tau^+\tau^-$ on $m_{t'}$ and ϕ_{sb} for different values of $|V^*_{t'b}V_{t's}|$.

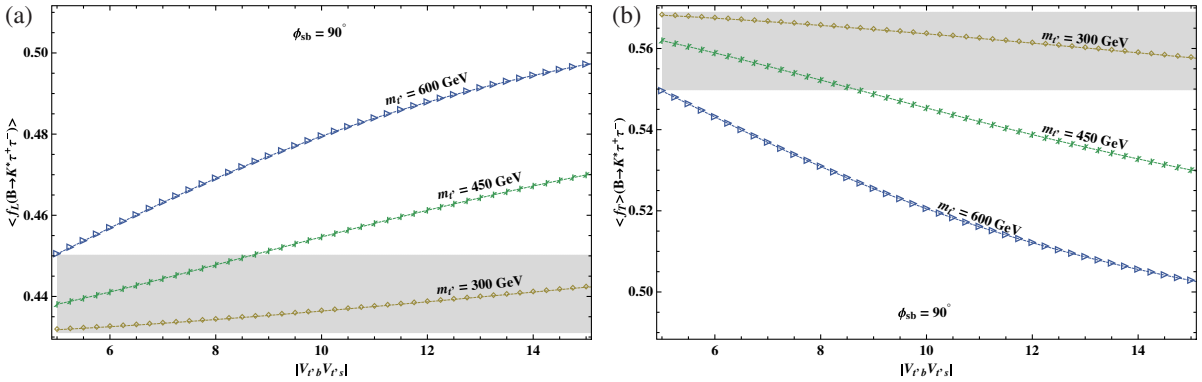

FIG. 10 (color online). The dependence of the average longitudinal and transverse helicity fractions for the decay $B \to K^*(892)\tau^+\tau^-$ on $|V^*_{t'b}V_{t's}|$ for different values of $m_{t'}$.

good observable to pin down the status of SM4. Moreover, we have also made the estimate of the average longitudinal helicity fraction of K^* meson in the low q^2 bin ($0.1 \le q^2 \le 6$ GeV^2) in the SM4 scenario as summarized in Table IV. One can compare these average values in the low q^2 bin with the experimental value given in Eqs. (24a)–(24d). With more data available from the LHCb we can use this information to put constraints on the SM4 parameter space.

(iii) In contrast to the case of muons, the helicity fractions are greatly influenced by SM4 when tauons are the final-state leptons as shown in Fig. 7. The effects of SM4 on the f_L and f_T are clearly distinct from the corresponding SM values in the low q^2 region, while the NP effects decreased in the high q^2 region. By taking a closer look at Figs. 7(b) and 7(d) one can extract that at the maximum values of $m_{t'} = 600$ GeV and $|V_{t'b}V_{t's}| = 0.015$, the shift in the minimum (maximum) values of the $f_T(f_L)$ is about 0.2, which lies at $q^2 = 4m_\tau^2$ and is well measured at experiments: this is a good observable to hunt the NP beyond the standard model.

(iv) Now, to qualitatively depict the effects of SM4 parameters on f_L and f_T for the decay $B \to K^*\tau^+\tau^-$, we have displayed their average values $<f_L>$ and $<f_T>$ as a function of $m_{t'}$, ϕ_{sb}, and $|V_{t'b}V_{t's}|$ in Figs. 8–10, respectively. These graphs indicate that the $<f_L>$ ($<f_T>$) is the increasing (decreasing) function of SM4 parameters. It is clear from Figs. 8(a), 8(b), 10(a), and 10(b) that when we set $\phi_{sb} = 90°$, $m_{t'} = 600$ GeV and $|V_{t'b}V_{t's}| = 0.015$, the value of $<f_L>$ ($<f_T>$) is enhanced (reduced) up (down) to 13% approximately. From Figs. 9(a) and 9(b) one can extract that at $\phi_{sb} = 120°$, $m_{t'} = 600$ GeV, and $|V_{t'b}V_{t's}| = 0.015$ this increment (decrement) in the $<f_L>$ ($<f_T>$) values reaches up to 16–17%, which is quite distinctive and to be observed at LHCb.

IV. SUMMARY

The polarization of K^* meson in the $B \to K^*\ell^+\ell^-$ ($\ell = \mu$ or τ) decay is studied from the perspective of SM4. In this respect, the polarized branching ratios BR_L, BR_T and the helicity fractions f_L, f_T of K^* meson are

studied. The explicit dependence of these observables on the $m_{t'}$, $|V_{t'b}V_{t's}|$ and ϕ_{sb} are also discussed. The study shows that the values of these observables are significantly affected by changing the value of SM4 parameters. As we discussed in the numerical analysis, the polarized branching ratios are directly proportional to the SM4 parameters $m_{t'}$ and $|V_{t'b}V_{t's}|$ and inversely proportional to the CKM4 phase ϕ_{sb} . It is found that at the maximum parametric space of SM4, the values of BR_L and BR_T are enhanced up to 6–7 times their SM values.

Similarly, the influence of SM4 parameters on helicity fractions f_L and f_T and their average values are studied. For the case of muons, these observables do not show any significant change in their SM values. However, for the case of tauns the effects are quite prominent and well-distinct from their SM values. The effects of SM4 on helicity fractions are decreased when the value of q^2 is increased and almost vanishes at the maximum value of q^2. It is also seen that the categorical influence of SM4 parameters $m_{t'}$, $|V_{t'b}V_{t's}|$ and ϕ_{sb} on $\langle f_L \rangle$ are constructive but destructive on $\langle f_T \rangle$. Therefore, the precise measurement of the observables related to the polarization of K^* meson, as discussed in this study, not only gave us an opportunity to test the SM it also was useful in finding out or putting some constraint on the SM4 parameters, such as $m_{t'}$, $|V_{t'b}V_{t's}|$ and ϕ_{sb}. It is also worth mentioning here that the SM4 effects are quite prominent in the low q^2 region, which is below the resonance region i.e. J/ψ and ψ-peaks region. However, for the case of tauons as a final-state leptons, the SM4 effects are distinct from the SM value above both resonance regions. To sum up, the precise study of the polarization of K^* meson at LHCb and Tevatron provide us with a handy tool for revealing the status of the extra generation of quarks.

ACKNOWLEDGMENTS

The authors would like to thank Professor Riazuddin, Professor Fayyazuddin, and Dr. Diego Tonelli for their valuable guidance and helpful discussions.

[1] Erin De Pree, G. Marshall, and Marc Sher, Phys. Rev. D, **80**, 037301 (2009)
[2] C. Amsler *et al.* (Particle Data Group), Phys. Lett. B **667**, 1 (2008).
[3] M. Maltoni, V. A. Novikov, L. B. Okun, A. N. Rozanov, and M. I. Vysotsky, Phys. Lett. B **476**, 107 (2000);H. J. He, N. Polonsky, and S. f. Su, Phys. Rev. D **64**, 053004 (2001); B. Holdom, Phys. Rev. D **54**, R721 (1996).
[4] G. D. Kribs, T. Plehn, M. Spannowsky, and T. M. P. Tait, Phys. Rev. D **76**, 075016 (2007).
[5] W. S. Hou and C. Y. Ma, Phys. Rev. D **82**, 036002 (2010).
[6] S. Bar-Shalom, D. Oaknin, and A. Soni, Phys. Rev. D **80**, 015011 (2009).
[7] A. J. Buras, B. Duling, T. Feldmann, T. Heidsieck, C. Promberger, and S. Recksiegel, J. High Energy Phys. 09 (2010) 106.
[8] A. Soni, A. K. Alok, A. Giri, R. Mohanta, and S. Nandi, Phys. Lett. B **683**, 302 (2010).
[9] O. Eberhardt, A. Lenz, and J. Rohrwild, Phys. Rev. D **82**, 095006 (2010).
[10] A. Soni, A. K. Alok, A. Giri, R. Mohanta, and S. Nandi, Phys. Rev. D **82**, 033009 (2010).
[11] A. K. Alok, A. Dighe, and D. London, Phys. Rev. D **83**, 073008 (2011).
[12] B. Holdom, Phys. Rev. Lett. **57**, 2496 (1986) ; **58**, 177 (1987).
[13] C. T. Hill, M. A. Luty, and E. A. Paschos, Phys. Rev. D **43**, 3011 (1991).
[14] T. Elliott and S. F. King, Phys. Lett. B **283**, 371 (1992).
[15] P. Q. Hung and C. Xiong, Nucl. Phys. B **848**, 288 (2011).
[16] B. Holdom, J. High Energy Phys. 08 (2006) 076.
[17] P. Q. Hung and M. Sher, Phys. Rev. D **77**, 037302 (2008).
[18] P. Q. Hung and C. Xiong, Phys. Lett. B **694**, 430 (2011).
[19] P. Q. Hung and C. Xiong, Nucl. Phys. **B847**, 160 (2011).
[20] O. Cakir, A. Senol, and A. T. Tasci, Europhys. Lett. **88**, 11002 (2009).
[21] B. Holdom, W. S. Hou, T. Hurth, M. L. Mangano, S. Sultansoy, and G. Unel, PMC Phys. A **3**, 4 (2009).
[22] T. Moroi, Phys. Lett. B **493**, 366 (2000).
[23] D. Chang, A. Masiero, and H. Murayama, Phys. Rev. D **67**, 075013 (2003).
[24] R. Harnik, D. T. Larson, H. Murayama, and A. Pierce, Phys. Rev. D **69**, 094024 (2004).
[25] M. Ciuchini, E. Franco, A. Masiero, and L. Silvestrini, Phys. Rev. D **67**, 075016 (2003).
[26] J. Foster, K.-i. Okumura, and L. Roszkowski, J. High Energy Phys. 08 (2005) 94.
[27] M. Blanke, A. J. Buras, B. Duling, S. Gori, and A. Weiler, J. High Energy Phys. 03 (2009) 001.
[28] M. Blanke, A. J. Buras, B. Duling, K. Gemmler, and S. Gori, J. High Energy Phys. 03 (2009) 108..
[29] M. Blanke *et al.*, J. High Energy Phys. 12 (2006) 003.
[30] V. Barger *et al.*, J. High Energy Phys. 12 (2009) 048.
[31] C. S. Kim *et al.*, Phys. Lett. B **218**, 343 (1989); X. G. He *et al.*, Phys. Rev. D **38**, 814 (1988); B. Grinstein *et al.*, Nucl. Phys. **B319**, 271 (1989); N. G. Deshpande *et al.*, Phys. Rev. D **39**, 1461 (1989); P. J. O'Donnell and H. K. K. Tung, Phys. Rev. D **43**, R2067 (1991); N. Paver and Riazuddin, Phys. Rev. D **45**, 978 (1992); J. L. Hewett, Phys. Rev. D **53**, 4964 (1996); T. M. Aliev, V. Bashiry, and M. Savci, Eur. Phys. J. C **35**, 197 (2004); T. M. Aliev, V. Bashiry, and M. Savci, Phys. Rev. D **72**, 034031 (2005); T. M. Aliev, V. Bashiry, and M. Savci, J. High Energy Phys. 05 (2004) 037; T. M. Aliev, V. Bashiry, and M. Savci, Phys. Rev. D **73**, 034013 (2006); T. M. Aliev, V. Bashiry, and M. Savci, Eur. Phys. J. C **40**, 505 (2005);

F. Kruger and L. M. Sehgal Phys. Lett. B **380**, 199 (1996); Y. G. Kim, P. Ko, and J. S. Lee, Nucl. Phys. **B544**, 64 (1999); Chuan-Hung Chen and C. Q. Geng, Phys. Lett. B **516**, 327 (2001); V. Bashiry, Chin. Phys. Lett. **22**, 2201 (2005); W. S. Hou, A. Soni, and H. Steger, Phys. Lett. B **192**, 441 (1987); W. S. Hou, R. S. Willey, and A. Soni, Phys. Rev. Lett. **58**, 1608 (1987); **60**, 2337(E) (1987); T. Hattori, T. Hasuike, and S. Wakaizumi, Phys. Rev. D **60**, 113008 (1999); T. M. Aliev, D. A. Demir, and N. K. Pak, Phys. Lett. B **389**, 83 (1996); Y. Dincer, Phys. Lett. B **505**, 89 (2001), and references therein; C. S. Huang, W. J. Huo, and Y. L. Wu, Mod. Phys. Lett. A **14**, 2453 (1999); C. S. Huang, W. J. Huo, and Y. L. Wu, Phys. Rev. D **64**, 016009 (2001); A. K. Alok *et al.*, J. High Energy Phys.02 (2010) 053.

[32] A. Ali, T. Mannel, and T. Morosumi, Phys. Lett. B **273**, 505 (1991).

[33] C. W. Chiang, R. H. Li, and C. D. Lü, arXiv:0911.2399.

[34] P. Colangelo, F. De Fazio, R. Feerandes, and T. N. Pham, Phys. Rev. D **74**, 115006 (2006).

[35] A. Ahmed, I. Ahmed, M. A. Paracha, and A. Rehman, Rev. Drug Metab. Drug Interact. **84**, 033010 (2011).

[36] T. M. Aliev, A. Ozpineci, and M. Savc, Phys. Lett. B **511**, 49 (2001).

[37] The LHCb Collaboration, in *2011 Europhysics Conference On High Energy Physics, France, 2011*, CERN-LHCb-CONF-2011-038, http://cdsweb.cern.ch/record/1367849?ln=en

[38] T. Aaltonen *et al.* (CDF Collaboration), arXiv:1108.0695 [Phys. Rev. Lett. (to be published)].

[39] J. T. Wei *et al.* (Belle Collaboration), Phys. Rev. Lett. **103**, 171801 (2009).

[40] B. Aubert *et al.* (BABAR Collaboration), Phys. Rev. D **79**, 031102(R) (2009).

[41] A. Ali, P. Ball, L. T. Handoko, and G. Hiller, Phys. Rev. D **61**, 074024 (2000).

[42] G. Buchalla, A. J. Buras, and M. E. Lautenbacher, Rev. Mod. Phys. **68**, 1125 (1996).

[43] A. J. Buras and M. Munz, Phys. Rev. D **52**, 186 (1995); A. J. Buras, M. Misiak, M. Munz, and S. Pokorski, Nucl. Phys. **B424**, 374 (1994).

[44] A. Ali, T. Mannel, and T. Morosumi, Phys. Lett. B **273**, 505 (1991).

[45] C. S. Kim, T. Morozumi, and A. I. Sanda, Phys. Lett. B **218**, 343 (1989).

[46] F. Kruger and L. M. Sehgal, Phys. Lett. **380**, 199 (1996).

[47] B. Grinstein, M. J. Savage, and M. B. Wise, Nucl. Phys. **B319**, 271 (1989).

[48] Cella and G. Ricciardi, and A. Vicere Phys. Lett. B **258**, 212 (1991).

[49] C. Bobeth, M. Misiak, and J. Urban, Nucl. Phys. **B574**, 291 (2000).

[50] H. H. Asatrian, H. M. Asatrian, C. Grueb, and M. Walker, Phys. Lett. B **507**, 162 (2001).

[51] M. Misiak, Nucl. Phys.**B393**, 23 (1993). **B439**, 461 (1995).

[52] T. Huber, T. Hurth, and E. Lunghi *The Role of Collinear Photons in the Rare Decay anti-B –> X(s) l+ l-* in (Les Rencontres de Moriond on QCD, Italy, 2008 and Flavor Physics and CP Violation (FPCP), Taiwan, 2008).

[53] A. Saddique, M. J. Aslam, and C. D. Lu, Eur. Phys. J. C **56**, 267 (2008).

[54] I. Ahmed, M. A. Paracha, M. Junaid, A. Ahmed, A. Rehman, and M. J. Aslam, arXiv:1107.5694.

[55] K. Nakamura *et al.* (Particle Data Group), J. Phys. G **37**, 075021 (2010).

[56] A. Soni *et al.*, Phys. Rev. D **82**, 033009 (2010).